Measurements of Higgs boson properties in ATLAS

Tim Adye, on behalf of the ATLAS Collaboration.
Particle Physics Department, Rutherford Appleton Laboratory, Didcot, United Kingdom

Combined measurements of the properties of the Higgs boson using the full pp collision data sample recorded in 2011–2012 by the ATLAS experiment at the LHC are presented. The combined mass measurement derived from the $H\to\gamma\gamma$ and $H\to ZZ^{(*)}\to 4\ell$ channels is $m_H = 125.5 \pm 0.2\,(\text{stat})\,^{+0.5}_{-0.6}\,(\text{sys})$ GeV. The signal strength, from the combination of the $H\to\gamma\gamma$, $H\to ZZ^{(*)}\to 4\ell$, and $H\to WW^{(*)}\to \ell\nu\ell\nu$ channels, as well as the $H\to\tau\tau$ and $H\to b\bar{b}$ channels using a partial dataset, is determined to be $\mu = 1.30\pm0.13\,(\text{stat})\pm0.14\,(\text{sys})$. The cross section ratio between vector boson mediated and gluon initiated Higgs boson production processes is found to be $\mu_{\text{VBF}+VH}/\mu_{\text{ggF}+t\bar{t}H} = 1.2^{+0.7}_{-0.5}$, with more than 3σ evidence for Higgs production through vector-boson fusion. Measurements of relative branching fraction ratios, as well as combined fits testing the fermion and vector boson couplings, ratio of couplings to W and Z, and the possible contribution of new particles show no significant deviation from the Standard Model expectation.

1 Introduction

The observation of a new particle in the search for the Standard Model (SM) Higgs boson at the LHC,[1] reported by the ATLAS[2,3] and CMS[4] Collaborations, is a milestone in the quest to understand electroweak symmetry breaking.[5–7] The ATLAS Collaboration has since reported first measurements of the particle's coupling properties,[8] and updated measurements of its signal strength[9] and mass.[10] Presented here[11,12] are new measurements of the mass, signal strengths, and coupling properties from a combination of decay modes using $4.8\,\text{fb}^{-1}$ of pp collision data at $\sqrt{s} = 7$ TeV and $20.7\,\text{fb}^{-1}$ at $\sqrt{s} = 8$ TeV for the three most sensitive channels $H\to\gamma\gamma$,[13,14] $H\to ZZ^{(*)}\to 4\ell$,[13,15] and $H\to WW^{(*)}\to \ell\nu\ell\nu$;[13,16] and using $4.8\,\text{fb}^{-1}$ at $\sqrt{s} = 7$ TeV and $13\,\text{fb}^{-1}$ at $\sqrt{s} = 8$ TeV for the $H\to\tau\tau$[17,18] and $H\to b\bar{b}$[17,19] channels.

2 Mass measurements

The mass of the new particle can be measured precisely from fits to the data for the $H\to\gamma\gamma$ and $H\to ZZ^{(*)}\to 4\ell$ channels: $m_H = 126.8 \pm 0.2\,(\text{stat}) \pm 0.7\,(\text{sys})$ GeV and $124.3^{+0.6}_{-0.5}\,(\text{stat})\,^{+0.5}_{-0.3}\,(\text{sys})$ GeV are found in the two cases, respectively.

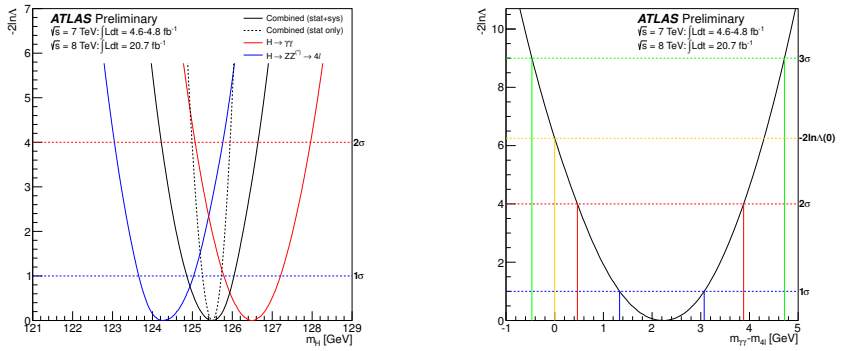

(a) (b)

Figure 1: The profile likelihood ratio $-2\ln\Lambda(m_H)$ as a function of (a) m_H and (b) the mass difference, $\Delta m_H = m_H^{\gamma\gamma} - m_H^{4\ell}$, for the $H\to\gamma\gamma$ and $H\to ZZ^{(*)}\to 4\ell$ channels and their combination. In both cases the signal strength parameters, $\mu_{\gamma\gamma}$ and $\mu_{4\ell}$, are allowed to vary independently.[11]

A combined measurement based on these two channels is obtained from the profile likelihood ratio $\Lambda(m_H)$,[20] as shown in Figure 1(a). The signal strength is allowed to vary between the two channels by treating $\mu_{\gamma\gamma}$ and $\mu_{4\ell}$ as independent nuisance parameters. The combined mass is measured to be $m_H = 125.5 \pm 0.2\,(\text{stat})\,^{+0.5}_{-0.6}\,(\text{sys})$ GeV.

To quantify the consistency between the fitted $m_H^{\gamma\gamma}$ and $m_H^{4\ell}$ values, the data are fitted with the profile likelihood ratio $\Lambda(\Delta m_H)$, where the parameter of interest is the mass difference $\Delta m_H = m_H^{\gamma\gamma} - m_H^{4\ell}$. The average mass m_H and the signal strengths $\mu_{\gamma\gamma}$ and $\mu_{4\ell}$ are treated as independent nuisance parameters. As shown in Figure 1(b), the resulting estimated mass difference is $\Delta\hat{m}_H = 2.3^{+0.6}_{-0.7}\,(\text{stat}) \pm 0.6\,(\text{sys})$ GeV. The probability of a single Higgs boson producing a value of $\Lambda(\Delta m_H)$ disfavoring the $\Delta m_H = 0$ hypothesis by more than that observed in the data is found to be 1.5% (2.4σ), using Monte Carlo ensemble tests.

The significance of the mass difference is also tested using rectangular pdfs for the systematic mass scale uncertainties coming from the $Z \to ee$ calibration procedure, the material upstream of the electromagnetic calorimeter, and the energy scale of the presampler detector. Rectangular pdfs give a flat *a priori* likelihood in the range of the quoted $\pm 1\sigma$ uncertainty intervals for these three sources and a zero probability outside this range. With this treatment, the consistency between the two mass measurements increases to 8% (1.7σ).

3 Signal strength

The Higgs boson production rate is measured in terms of the signal strength parameter μ, a scale factor with respect to the SM predicted rate. The observed overall signal strength μ is determined from a fit to the data where all channels are combined, using the profile likelihood ratio $\Lambda(\mu)$. The mass is fixed to the measured value $m_H = 125.5$ GeV. Figure 2(a) shows the measured signal strengths for the individual channels as well as their combination, $\hat{\mu} = 1.30 \pm 0.13\,(\text{stat}) \pm 0.14\,(\text{sys})$.

The compatibility between this measurement and the SM Higgs boson expectation ($\mu = 1$) is about 9%. It increases to about 40% if rectangular pdfs are used for the dominant theoretical systematic uncertainties from the $gg \to H$ QCD scale and PDF variations. The overall compatibility between the signal strengths measured in the five individual channels and their SM predictions is about 8%. The compatibility between the measured individual $\hat{\mu}$ values and their combination is 13%. The dependence of the combined value of $\hat{\mu}$ on the assumed m_H is relatively weak: changing the mass hypothesis by ± 1 GeV changes $\hat{\mu}$ by about ± 4%.

In order to test which values of signal strength and Higgs mass are simultaneously consistent with the data for the $H\to\gamma\gamma$ and $H\to ZZ^{(*)}\to 4\ell$ channels, the profile likelihood ratio $\Lambda(\mu, m_H)$

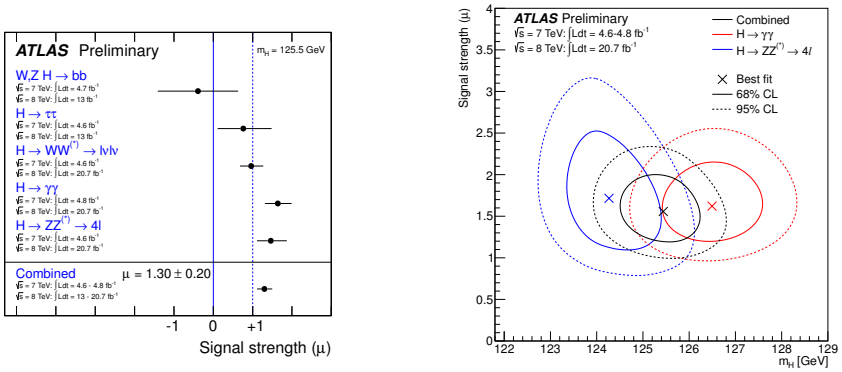

(a) (b)

Figure 2: (a) Measurements of the signal strength parameter μ at $m_H = 125.5$ GeV for the individual channels and their combination.[12] (b) Confidence level intervals in the (μ, m_H) plane for the $H\to ZZ^{(*)}\to 4\ell$ and $H\to\gamma\gamma$ channels and their combination, including all systematic uncertainties. The markers indicate the maximum likelihood estimates $(\hat{\mu}, \hat{m}_H)$ in the corresponding channels.[11]

is used. The resulting 68% and 95% CL contours are shown in Figure 2(b).

4 Production and decay modes

The signal strengths of different production processes contributing to the same final state are determined, exploiting the sensitivity offered by the use of event categories in the analyses of each channel.

The data are fitted separating vector-boson-mediated processes (VBF and VH) from gluon-initiated processes (ggF and ttH) involving fermions (mainly top-quark loops). The signal strength parameters, $\mu_{\mathrm{ggF}+t\bar{t}H} = \mu_{\mathrm{ggF}} = \mu_{t\bar{t}H}$ and $\mu_{\mathrm{VBF}+VH} = \mu_{\mathrm{VBF}} = \mu_{VH}$, are measured for each of the final states, $H\to\gamma\gamma$, $H\to ZZ^{(*)}$ $H\to WW^{(*)}\to\ell\nu\ell\nu$, and $H\to\tau\tau$, as shown in Figure 3(a).

The combination of these results can be made in a model-independent way (i.e. without assumptions on the Higgs decay branching ratios) by measuring the ratio, $\mu_{\mathrm{VBF}+VH}/\mu_{\mathrm{ggF}+t\bar{t}H} = 1.2^{+0.7}_{-0.5}$. The results of the fit to the data for the individual channels and their combination are shown in Figure 3(b). Good agreement with the SM expectations is observed.

To test the sensitivity to VBF production alone, the data are also fitted with the ratio $\mu_{\mathrm{VBF}}/\mu_{\mathrm{ggF}+t\bar{t}H}$, profiling μ_{VH}. From the combination of the four channels, the same value of $\mu_{\mathrm{VBF}}/\mu_{\mathrm{ggF}+t\bar{t}H} = 1.2^{+0.7}_{-0.5}$ is obtained. This result provides 3.1σ evidence for VBF production, with the p-value for vanishing VBF being 0.09%.

Conversely, to study the decay modes independently of the production modes, the ratio of branching ratios, relative to their SM expectations are studied. The best-fit values for each decay mode ratio is $\rho_{\gamma\gamma/ZZ} = 1.1^{+0.4}_{-0.3}$, $\rho_{\gamma\gamma/WW} = 1.7^{+0.7}_{-0.5}$, and $\rho_{ZZ/WW} = 1.6^{+0.8}_{-0.5}$, all in agreement with the SM expectation of 1.

5 Higgs couplings

A relative coupling, κ_i, is defined as the ratio of the measured coupling to the SM one. For each observed final state of the SM Higgs boson, the production and decay rates involve several couplings. For example in the $gg\to H\to\gamma\gamma$ mode, the production rate from gluon fusion is proportional to the square of the effective Higgs-gluon coupling, κ_g^2, where κ_g is itself a function of the Higgs couplings to the particles running in the loops, principally the top, κ_t. The diphoton decay rate is proportional to the square of the effective photon coupling, κ_γ^2, itself a function of κ_W and κ_t, describing the interference between the W and top loops. The data do not

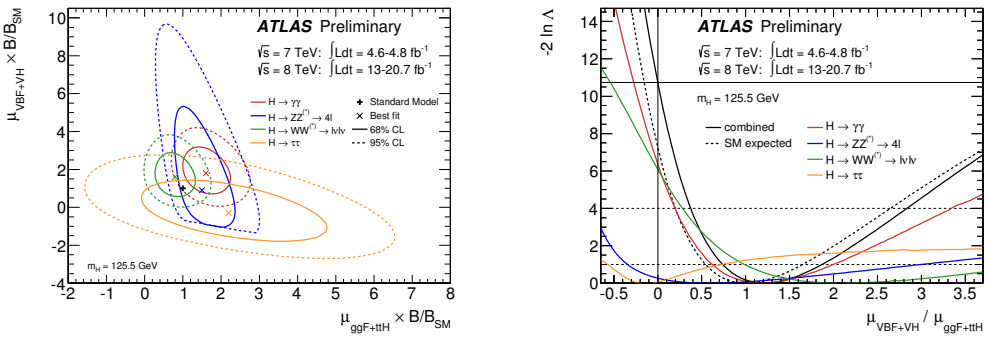

(a) (b)

Figure 3: (a) Likelihood contours for the $H\to\gamma\gamma$, $H\to ZZ^{(*)}\to 4\ell$, $H\to WW^{(*)}\to \ell\nu\ell\nu$, and $H\to\tau\tau$ channels in the $(\mu_{\mathrm{ggF}+t\bar{t}H}, \mu_{\mathrm{VBF}+VH})$ plane. Both $\mu_{\mathrm{ggF}+t\bar{t}H}$ and $\mu_{\mathrm{VBF}+VH}$ are modified by the decay mode-specific branching ratio factors $\mathrm{B/B_{SM}}$. (b) Likelihood curves for the ratio $\mu_{\mathrm{VBF}+VH}/\mu_{\mathrm{ggF}+t\bar{t}H}$ for these channels and their combination (observed and SM expectation).[12]

allow a complete determination of all the elementary couplings, so a few benchmark models are considered.[21]

5.1 Fermion versus vector couplings

In this model, all fermion (relative) couplings are taken equal ($\kappa_F = \kappa_\mathrm{t} = \kappa_\mathrm{b} = \kappa_\tau$), as are the vector boson couplings ($\kappa_V = \kappa_\mathrm{W} = \kappa_\mathrm{Z}$). The model assumes that $gg \to H$ production and $H\to\gamma\gamma$ decays occur only through loops of SM particles and that there are no non-SM decays contributing to the total width (additional models, measuring $\lambda_{FV} = \kappa_F/\kappa_V$, allow these assumptions to be relaxed[12]). Figure 4(a) shows the corresponding likelihood contours in the κ_V,κ_F plane. The relative sign between κ_F and κ_V corresponds to the interference of the top and W loops in $H\to\gamma\gamma$ decays, where $\kappa_V > 0$ by convention and $\kappa_F < 0$ would indicate a non-SM interference. The 68% CL intervals, profiling over the other parameter, are $\kappa_V \in [0.91, 0.97]\cup[1.05, 1.21]$ and $\kappa_F \in [-0.88, -0.75]\cup[0.73, 1.07]$, with the SM-like minimum, $\kappa_F > 0$, slightly favoured. The (2D) compatibility with the SM hypothesis 8%.

5.2 W and Z couplings (custodial symmetry)

Identical coupling scale factors for the W and Z are an important ingredient of the SM, often referred to as custodial symmetry. From the previous model with the total width free, κ_W and κ_Z are now separated, and their ratio, λ_WZ, is probed. Figure 4(b) shows the likelihood curve for λ_WZ, while profiling $\lambda_{F\mathrm{Z}} = \kappa_F/\kappa_\mathrm{Z}$ and $\kappa_{\mathrm{ZZ}} = \kappa_\mathrm{Z}\cdot\kappa_\mathrm{Z}/\kappa_\mathrm{H}$ in the fit. The 68% CL interval is $\lambda_\mathrm{WZ} \in [0.64, 0.87]$, with a (3D) compatibility with the SM hypothesis of 5%.

5.3 Contribution from non-SM particles

This model assumes that all couplings take their SM values ($\kappa_i = 1$), but the effective couplings to gluons and photons, κ_g and κ_γ, are taken as independent, allowing for additional contributions from new particles in the loops. As a first step, the model assumes that these particles do not contribute to the total width through invisible or undetected decay modes. Figure 4(c) shows the likelihood contours in the κ_g,κ_γ plane. The best fit values, profiling over the other parameter, are $\kappa_\mathrm{g} = 1.08 \pm 0.14$ and $\kappa_\gamma = 1.23^{+0.16}_{-0.13}$. The (2D) compatibility with the SM hypothesis is 5%.

In a second step, the assumption on the total width is released. The free parameters are κ_g, κ_γ, and $\mathrm{BR_{inv.,undet.}}$, where the latter represents the branching ratio to possible invisible and undetected decay modes. Figure 4(d) shows the likelihood as a function of $\mathrm{BR_{inv.,undet.}}$, profiling

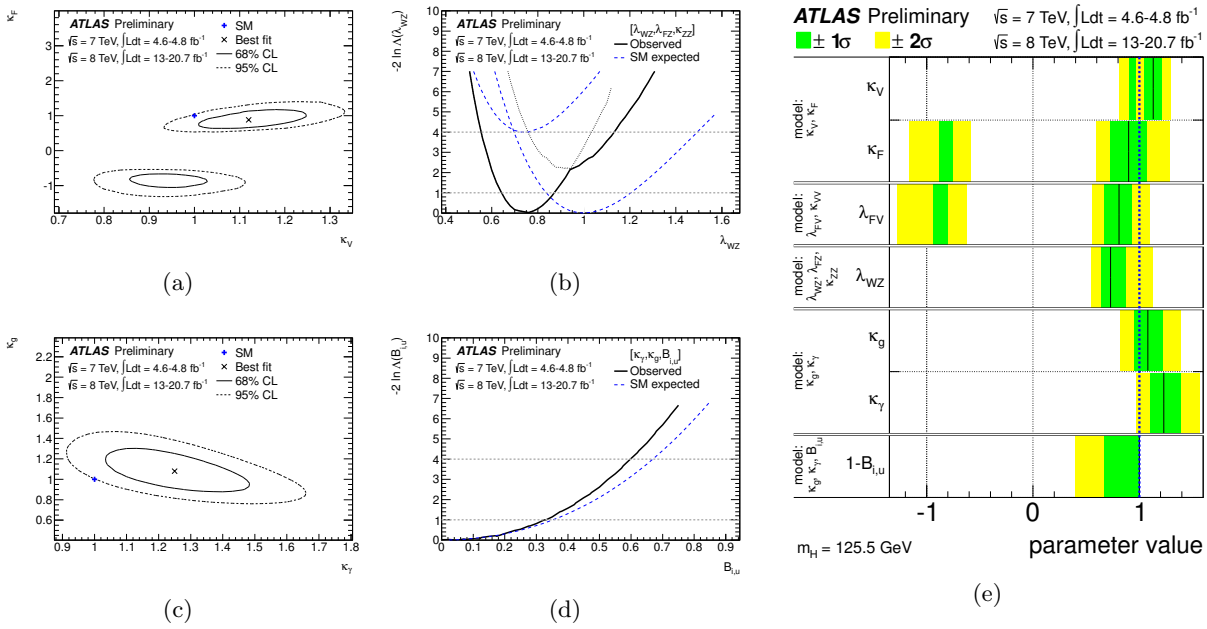

Figure 4: Fits to four benchmark coupling models: likelihood contours for (a) κ_F and κ_V (fermion and vector couplings) and (c) κ_g and κ_γ (effective $gg \to H$ and $H \to \gamma\gamma$ couplings); and likelihood curves for (b) $\lambda_{WZ} = \kappa_W/\kappa_Z$ (couplings to W and Z) and (d) $BR_{inv.,undet.}$ (branching fraction to invisible or undetectable decay modes). The dashed curves in (b) and (d) show the SM expectation. The thin dotted lines in (b) indicate the continuation of the likelihood curve when restricting the parameters to either the positive or negative sector of λ_{FZ}. (e) Summary of the coupling scale factor measurements. The best-fit values are represented by the solid vertical lines. The measurements in the different coupling benchmark models are strongly correlated, as they are obtained from fits to the same experimental data. They should not be considered as independent measurements.[12]

over κ_g and κ_γ. The 95% CL upper limit is $BR_{inv.,undet.} < 0.6$, with a (3D) compatibility with the SM hypothesis of 10%.

6 Conclusion

An update of the properties of the newly discovered Higgs-like boson using the full 2011–2012 data set for the three most sensitive channels $H \to \gamma\gamma$, $H \to ZZ^{(*)} \to 4\ell$ and $H \to WW^{(*)} \to \ell\nu\ell\nu$ is presented.

The measured mass, based on fits to the spectra of the $H \to \gamma\gamma$ and $H \to ZZ^{(*)} \to 4\ell$ channels, is $m_H = 125.5 \pm 0.2\,(\text{stat})\,^{+0.5}_{-0.6}\,(\text{sys})$ GeV. The difference of the mass measurements between the two channels is $2.3^{+0.6}_{-0.7}\,(\text{stat}) \pm 0.6\,(\text{sys})$ GeV, corresponding to a probability of a common mass of 1.5% (2.4σ) or 8% (1.7σ), depending on the treatment of mass scale systematic uncertainties.

A combined strength of $\hat{\mu} = 1.30 \pm 0.13\,(\text{stat}) \pm 0.14\,(\text{sys})$ is obtained. The cross section ratio between vector-boson mediated and gluon initiated Higgs boson production processes is determined to be $\mu_{\text{VBF}+VH}/\mu_{\text{ggF}+t\bar{t}H} = 1.2^{+0.7}_{-0.5}$, with 3.1σ evidence for VBF production.

The compatibility of the measurements with the SM Higgs boson predictions is tested using various coupling models. A summary of all coupling scale factor measurements is shown in Figure 4(e), all being compatible with the SM Higgs expectation at the 5–10% level. No significant deviation from the SM prediction is observed in any of the fits performed.

References

1. L. Evans and P. Bryant, JINST **3** no. 08, (2008) S08001.
2. ATLAS Collaboration, JINST **3** (2008) S08003.
3. ATLAS Collaboration, Phys. Lett. **B 716** (2012) 1, arXiv:1207.7214 [hep-ex].

4. CMS Collaboration, Phys. Lett. **B 716** (2012) 30, arXiv:1207.7235 [hep-ex].
5. F. Englert and R. Brout, Phys. Rev. Lett. **13** (1964) 321–323.
6. P. W. Higgs, Phys. Rev. Lett. **13** (1964) 508–509.
7. G. S. Guralnik, C. R. Hagen, and T. W. B. Kibble, Phys. Rev. Lett. **13** (1964) 585–587.
8. ATLAS Collaboration, ATLAS-CONF-2012-127 (2012).
9. ATLAS Collaboration, ATLAS-CONF-2012-162 (2012).
10. ATLAS Collaboration, ATLAS-CONF-2012-170 (2012).
11. ATLAS Collaboration, ATLAS-CONF-2013-014 (2013).
12. ATLAS Collaboration, ATLAS-CONF-2013-034 (2013).
13. E. Mountricha, *these proceedings*.
14. ATLAS Collaboration, ATLAS-CONF-2013-012 (2013).
15. ATLAS Collaboration, ATLAS-CONF-2013-013 (2013).
16. ATLAS Collaboration, ATLAS-CONF-2013-030 (2013).
17. D. Puigh, *these proceedings*.
18. ATLAS Collaboration, ATLAS-CONF-2012-160 (2012).
19. ATLAS Collaboration, ATLAS-CONF-2012-161 (2012).
20. G. Cowan, K. Cranmer, E. Gross, and O. Vitells, Eur. Phys. J. **C71** (2011) 1554.
21. LHC Higgs Cross Section Working Group, A. David *et al.*, LHCHXSWG-2012-001 (2012), arXiv:1209.0040 [hep-ph].